RESEARCH ARTICLE

Concentration-dependent Self-assembly of an Unusually Large Hexameric Hydrogen-bonded Molecular Cage

Severin Merget[a], Lorenzo Catti[b], Shani Zev[c], Dan T. Major[c], Nils Trapp[d] and Konrad Tiefenbacher*[a, e]

[a] M. Sc. S. Merget., Prof. Dr. K. Tiefenbacher
Department of Chemistry,
University of Basel
Mattenstrasse 24a, CH-4058 Basel, Switzerland
E-mail: konrad.tiefenbacher@unibas.ch, tkonrad@ethz.ch
[b] Dr. L. Catti,
WPI Nano Life Science Institute (WPI-NanoLSI),
Kanazawa University
Kakuma-machi, Kanazawa 920-1192, Japan
[c] Prof. Dr. D. T. Major
Department,of Chemistry and Institute for Nanotechnology & Advanced Materials
Bar-Ilan University
Ramat-Gan 52900, Israel
[d] Dr. N. Trapp
Laboratorium für Organische Chemie
ETH Zurich,
Vladimir-Prelog-Weg 3, CH-, 8093, Zürich, Switzerland
[e] Prof. Dr. K. Tiefenbacher
Department of Biosystems Science and Engineering,
ETH Zürich
Mattenstrasse 26, CH-4058 Basel, Switzerland

Supporting information for this article is given via a link at the end of the document.

Abstract: The sizes of available self-assembled hydrogen bond based supramolecular capsules and cages are rather limited. The largest systems feature volumes of approx. 1400 − 2300 Å^3. Here, we report a large, hexameric cage based on intermolecular amide–amide dimerization. The unusual structure with openings, reminiscent of covalently linked cages, is held together by 24 hydrogen bonds. With a diameter of 2.3 nm and a cavity volume of ~ 2800 Å^3 the assembly is larger than any previously known capsule/cage structures relying exclusively on hydrogen bonds. The self-assembly process in chlorinated, organic solvents was found to be strongly concentration dependent with the monomeric form prevailing at low concentrations. Additionally, the formation of host–guest complexes with fullerenes (C_{60} and C_{70}) was observed.

Introduction

The self-assembly of molecular capsules and cages using noncovalent interactions like hydrogen bonds,[1, 2] halogen bonds[3] or hydrophobic interactions[4] has been studied intensively over the last decades. Interestingly, in the case of hydrogen bond based systems, the size of the assemblies formed remained rather modest. The octameric capsule (Fig. 1a), reported by the *Mastalerz* group in 2016 constitutes the largest structure with a diameter of approx. 1.8 nm (V ~ 2300 Å^3).[2b]

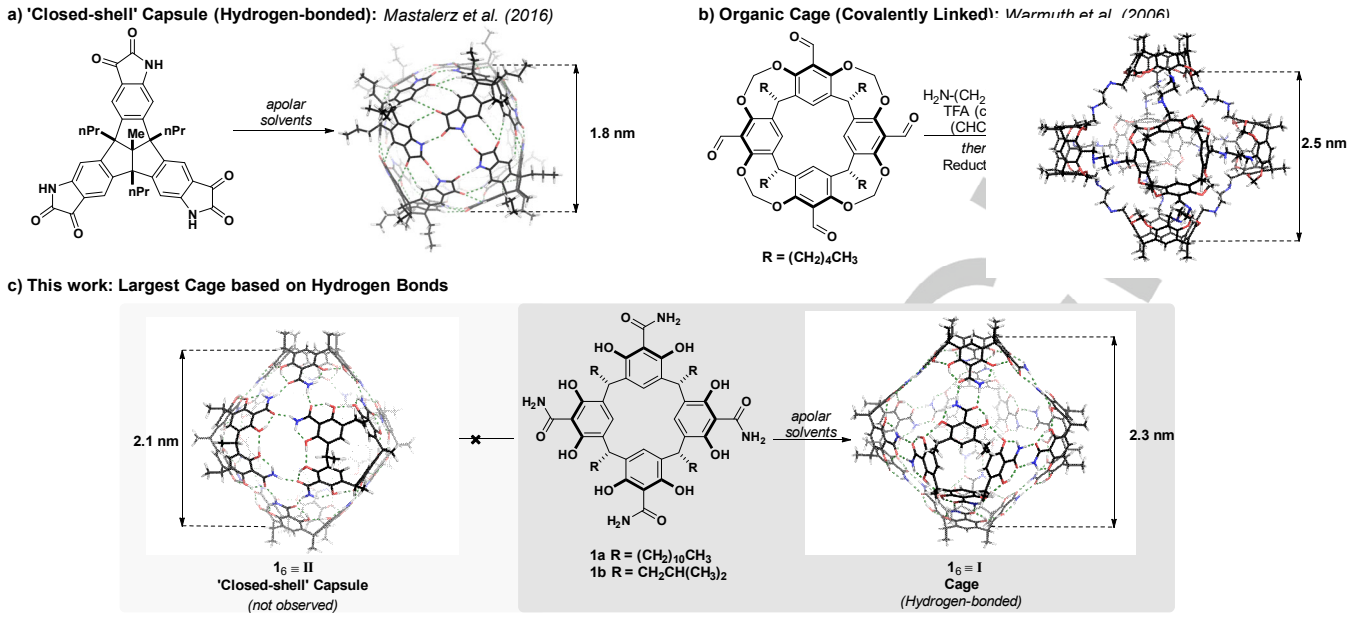

Figure 1. Molecular models of a) the octameric structure reported by *Mastalerz*, b) the covalently linked cage reported by *Warmuth* and c) the herein reported structure **I**, assembled from six units of **1a** (R residues are omitted for clarity).

In contrast, the self-assembly of cages *via* covalent bonds[5] and especially metal–ligand interactions[6] has furnished much larger structures with volumes of up to 157000 Å^3 and more than a hundred components.[7] What causes this size discrepancy? Metal–ligand self-assembly is highly predictable concerning the number of ligands binding to the metal center and the angle between these ligands. In contrast, hydrogen bonding is less predictable. While a linear binding mode is ideal, large deviations are tolerated. Moreover, different binding motives can be observed (f.i. bifurcation of the hydrogen bond) that can further complicate a rational design. Most importantly, however, the linearity of the hydrogen bond requires the design and synthesis of curved building blocks, while in the case of metal–ligand self-assembly the curvature can be imparted by the metal binding site. These factors reduce the predictability of the self-assembly process *via* hydrogen bonds, and in many cases the formation of extended networks is observed.[2b, 8] These problems can be overcome to a large extent by designing dimeric systems.[1, 9] Unfortunately, the synthetic effort usually scales with the size of the building blocks, rendering this approach challenging when trying to obtain larger assemblies. Among the noteworthy exceptions are the hexameric resorcinarene[10] and pyrogallolarene[11] capsules (d ~ 1.8 nm; V ~ 1400 Å^3), the Stefankiewicz[2c] capsule (d ~ 1.9 nm; V ~ 1700 Å^3) and the largest example by the Mastalerz group[2b] (d ~ 1.8 nm; V ~ 2300 Å^3) already mentioned before (Figure 1a).

Another striking feature of most multimeric assemblies based on hydrogen bonding is the formation of a 'closed-shell' capsule, effectively isolating the interior from the surrounding solvent. This is in stark contrast to metal–ligand based[5] and covalently linked cages[6] many of which have large openings. Such open structures are of interest not only since the pores potentially offer an additional binding site, but also because they allow small molecules to diffuse in and out of the cavity without the need for partial disassembly required for closed-shell capsules. Furthermore, the pores potentially offer the possibility for further modification of the assembly. *Warmuth* and co-workers have pioneered the assembly of covalent organic cages based on methylene bridged resorcinarene derivatives.[12] (Figure 1b). The cages are formed using dynamic covalent imine chemistry and feature openings of considerable size (d ~ 8 Å). The approach[13] has been extended towards chiral hydrazone cages by *Szumna* and co-workers using resorcinarene derivatives with unfunctionalized phenol groups.[14]

In order to construct a very large assembly based on hydrogen bonds we decided to synthesize the tetraamide-functionalized resorcinarene **1a** (Fig. 1c). Interestingly, this building block would be suited to self-assemble into two structurally very different hexameric structures, according to our initial molecular modelling. A direct amide–amide dimerization would form an unusually large cage structure **I**, while an amide trimerization binding motive would form a smaller closed-shell capsule **II** (Fig. 1c).

Herein, we present our results concerning the self-assembly of the organic cage **I** with an internal cavity volume of ~ 2800 Å^3 – to the best of our knowledge the largest cage structure that relies solely on hydrogen bonding.

Results and Discussion

First, a reliable synthetic route to macrocycle **1a** had to be developed (Figure 2a). Starting from resorcinarene, the tetrabrominated compound **2a** was accessible on the decagram scale *via* bromination and methylation following a literature procedure.[15] Initial attempts to access tetraamide **3a** from **2a** *via* cyanide coupling followed by hydrolysis proved futile, due to the unreactive nature of the nitrile compound. Ultimately, the introduction of the four amide moieties was achieved in 47% yield by treatment of **2a** with an excess of *n*-butyllithium, followed by

addition of trimethylsilyl isocyanate (TMSNCO) as the electrophile. Finally, the methyl protecting groups were removed with trimethylsilyl iodide (TMSI) to yield macrocycle **1a** in 74% yield. Derivative **1b** featuring shorter *iso*-butyl chains was synthesized along the same route and used for X-ray structure analysis (see SI for details).

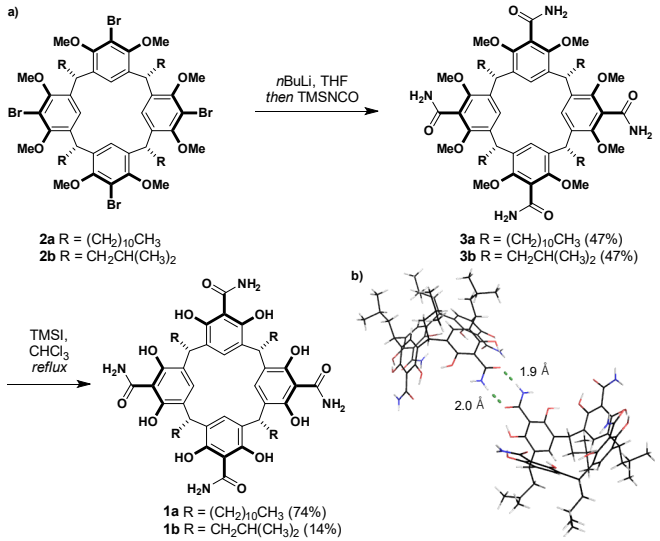

Figure 2. a) Synthesis of **1a** and 1**b** starting from **2a** and **2b**, respectively. b) Representation of the wave-like crystal structure of **1b** obtained from diethylether/nitrobenzene. Solvent molecules were omitted for clarity.

Crystals were obtained by slow evaporation of a saturated solution of **1b** in diethylether/nitrobenzene (10/1) at room temperature. Two types of structures were identified, using this protocol. Occasionally, **1b** crystallized forming a wave-like structure (Figure 2b) that could be solved using small molecule methods and was also found when employing other solvents (i.e. toluene) for crystallization. In this structure the intermolecular amide–amide hydrogen bonding is evident with measured NH – O=C distances of 1.9 – 2.0 Å.[16] In most cases however, the crystals obtained showed a much larger cubic unit cell (a = 3.7 nm) with a maximum resolution of 1.2 Å, suggesting a large self-assembled structure. Unfortunately, disordered solvent molecules within the cavity prevented solving of this larger structure with small molecule methods.

Although macrocycle **1a** contains several polar groups on its upper rim it was found to be well soluble (≥ 50 µmol/mL, ≥ 64 mg/mL) in apolar, chlorinated solvents (i.e. $CDCl_3$, CD_2Cl_2, tetrachloroethane-d_2 (TCE-d_2)) as well as aromatic solvents (C_6D_6, toluene-d_8). The relevant low-field regions of the ^{1}H-NMR spectra in different solvents, including acetone-d_6 that prevents hydrogen bond based self-assembly, are displayed in Figure 3. The spectra in apolar solvents show largely similar features: (i) the two amide NH-protons (C and D) resonate at a similar chemical shift in the range of 8.50 – 9.50 ppm, indicating that they both participate in the hydrogen bond network; (ii) the protons corresponding to the phenol groups (A and B) differ quite significantly with proton A (16.0 – 17.0 ppm) being highly deshielded due to the hydrogen bond with the neighboring carbonyl group, while proton B (9.70 – 10.8 ppm) forms a hydrogen bond with the phenol-group at the adjacent aromatic ring and experiences a weaker downfield shift (see SI for 2D-NMR data). All major peaks correspond to a single diffusing entity (D = 2.39 ± 0.005 × 10^{-10} m^2/s in $CDCl_3$ (5 mM)) as indicated by DOSY-NMR in different solvents (see SI). The hydrodynamic radius (r_h) in apolar solvents was estimated to be 1.81 – 1.96 nm, which indicates an assembly of higher order [2b, 17] similar in size to previously reported hexameric structures.[18] The spectrum of **1a** (20 mM) in $CDCl_3$ as wells as TCE-d_2, features additional small peaks and shoulders next to the OH signals (A and B) and at 5.84 ppm (red dots in Figure 3), beside the main peaks (green dots). We found the ratio between the main peaks and these smaller signals to be highly dependent on the concentration of the NMR sample (Figure 4b). Furthermore, DOSY-NMR spectra revealed a significantly higher diffusion coefficient of the signals marked with the red dots (D = 3.53 ± 0.021 × 10^{-10} m^2/s (5 mM in $CDCl_3$)) indicating a much smaller species (Figure 4d). Upon varying the concentration, it became evident that at low concentration the small species is preferred while at high concentration the hexameric structure **I** is formed predominantly (Figure 4c). The strong upfield shift from 8.98 to 5.78 ppm of NH-proton C' (highlighted in red in Fig. 4b) indicates the loss of a strong hydrogen bond in the smaller species as compared to the larger one.[19] The loss of a strong hydrogen bond at atom C' indicates that the smaller species is the monomeric species **1a**. In the hexameric structure, one of the NH-protons (C) forms an intermolecular hydrogen bond with the carbonyl moiety of a second macrocycle leading to a significant deshielding. This hydrogen bond is lost in the monomeric species and the NH-proton (C') experiences an upfield shift. [20]

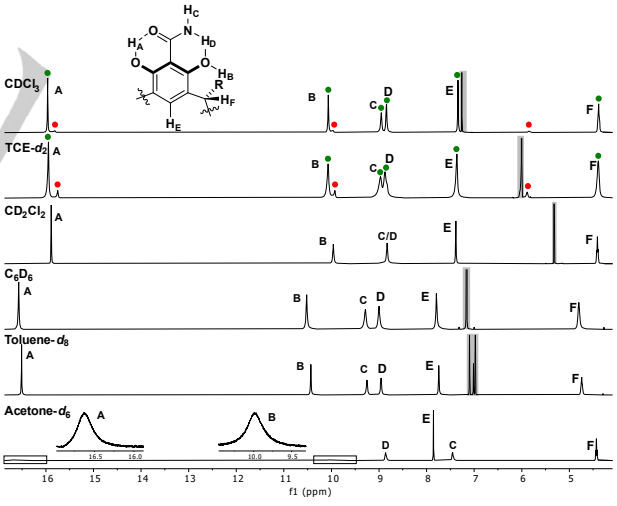

Figure 3. Partial ^{1}H-NMR spectra of **1a** (20 mmol/L) in different solvents. Signals corresponding to the main species **I** are marked with a green dot (●). Signals corresponding to the monomeric species **1a** are marked with a red dot (●). Solvent peaks are marked in grey.

In contrast, the chemical environment of the protons involved in intramolecular hydrogen bonds (A', B', D'$H_{A'}$, $H_{B'}$, $H_{D'}$) remains rather similar and only a small shift is observed at different concentrations.

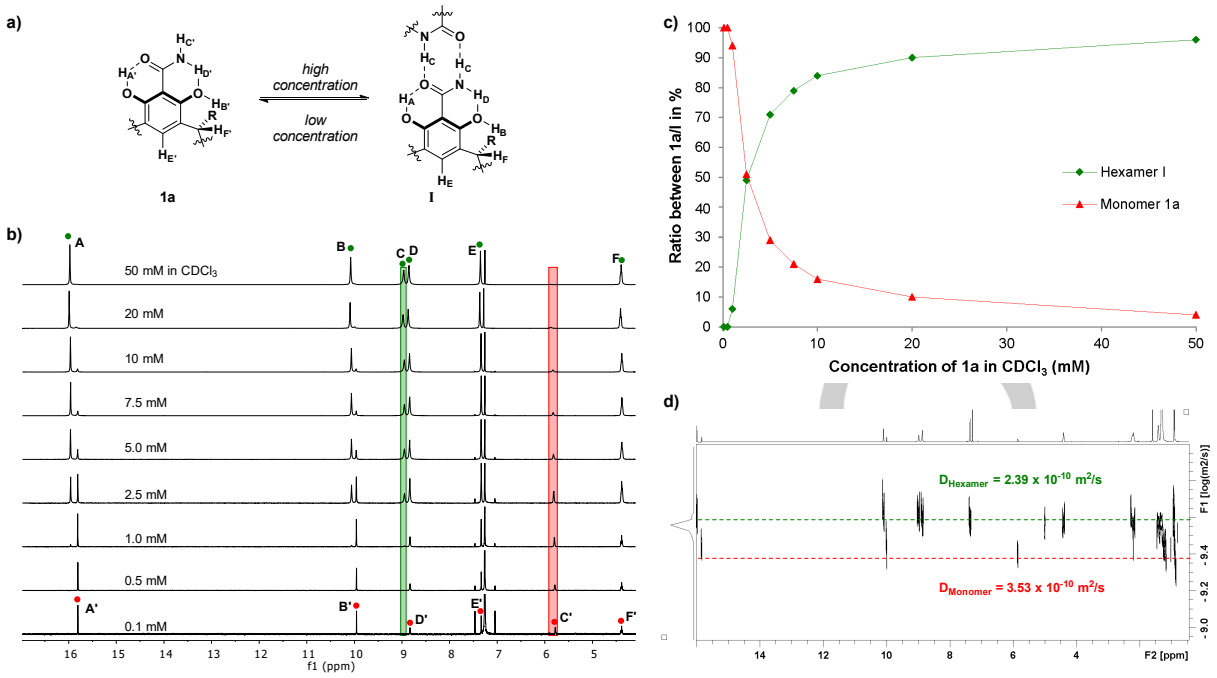

Figure 4. a) Concentration dependent assembly process between monomer **1a** (red ●) and hexamer **I** (green ●) in apolar solvents. b) Partial ^{1}H-NMR spectra of **1a**/**I** in $CDCl_3$ at different concentrations (0.1 – 50 mM based on **1a**). c) Ratio between monomer **1a** and hexamer **I** as a function of the monomer concentration. d) DOSY-NMR spectrum of **1a**/**I** (5.0 mM) showing the different diffusion coefficients for **1a** and **I**.

Similar trends are observed in the acetone-d_6 solution of **1a** (Figure 3), as the self-assembly process is suppressed by the solvent. The spectrum is in fact comparable to the one of **1a** in $CDCl_3$ at lower concentration (Figure 4b), although the difference for the two NH-protons (C' and D') is not as pronounced in acetone-d_6; presumably because proton C' still experiences some deshielding due to hydrogen bonding with the solvent. Varying the concentration of **1a** in TCE-d_2 and CD_2Cl_2 (see SI) as well as in aromatic solvents (C_6D_6, toluene-d_8) led to similar results concerning a second smaller species prevailing at low concentration.

Interestingly, a study concerning the self-assembly of the pyridinearene macrocycle **4** (Figure 5a) by *Cohen* and co-workers[18c] revealed analogous behavior. Also in this case two species were distinguished by DOSY-NMR in $CDCl_3$: a large hexameric capsule ($D = 2.36 \times 10^{-10}$ m^2/s) and a smaller species ($D = 3.50 \times 10^{-10}$ m^2/s in $CDCl_3$) assigned as a dimer. Addition of TFA (trifluoroacetic acid) led to disassembly and allowed the observation of the monomer in solution ($D = 4.31 \times 10^{-10}$ m^2/s).

In our case the diffusion coefficients of both species **1a** and **I** were found to be concentration dependent (Figure 5b). At low concentrations, where the assembled species **I** is effectively absent, the diffusion coefficient of the small species increases to reach values of up to 4.83×10^{-10} m^2/s (1.0 mM in $CDCl_3$) with decreasing concentration, which is in good agreement with values previously reported for pyridinearene **4** in its monomeric form. To obtain an independent reference for the monomeric form the globally methyl protected resorcinarene derivative **5** was used, which cannot self-assemble. Macrocycle **5** was accordingly found to have a diffusion coefficient of 4.86×10^{-10} m^2/s (5.0 mM in $CDCl_3$), which is in good agreement with the value obtained for **1a** at low concentration. In contrast, at high concentrations the assembled species **I** prevails and the diffusion coefficient decreases to reach 1.71×10^{-10} m^2/s at 50 mM in $CDCl_3$ indicating the formation of a large, discrete assembly. As the decreasing diffusion coefficient might be simply caused by an increase in viscosity at higher macrocycle concentrations, we compared the behavior to the well-known resorcinarene[10] and pyrogallolarene[11] hexamers assembling from macrocycles **6** and **7**, respectively (Figure 5c). In all cases the diffusion coefficient decreases at higher concentration, however, the effect is much more pronounced for macrocycle **1a** which indicates that indeed the hexamer **I** is significantly larger than the resorcinarene and pyrogallarene based hexamers. Assuming that for all assemblies the contribution of the alkyl feet is similar, the hydrodynamic radius determined from the respective diffusion coefficient (measured at 50 mM) correlates very well with the molecular models (Table S4). For the resorcinarene hexamer (r_h = 1.99 nm; estimated r = 2.01 nm) and the pyrogallolarene hexamer (r_h = 1.91 nm; estimated r = 1.97 nm), an excellent correlation was observed. Also the proposed structure of cage-like hexamer **I** (r_h = 2.36 nm) displays a very good fit to the molecular model (estimated r = 2.39 nm). As the alternative closed-shell structure **II** does not match the observed hydrodynamic radius, we excluded this option. In conclusion, the DOSY-NMR investigations provided evidence that strongly support the formation of the cage-like hexamer **I**.

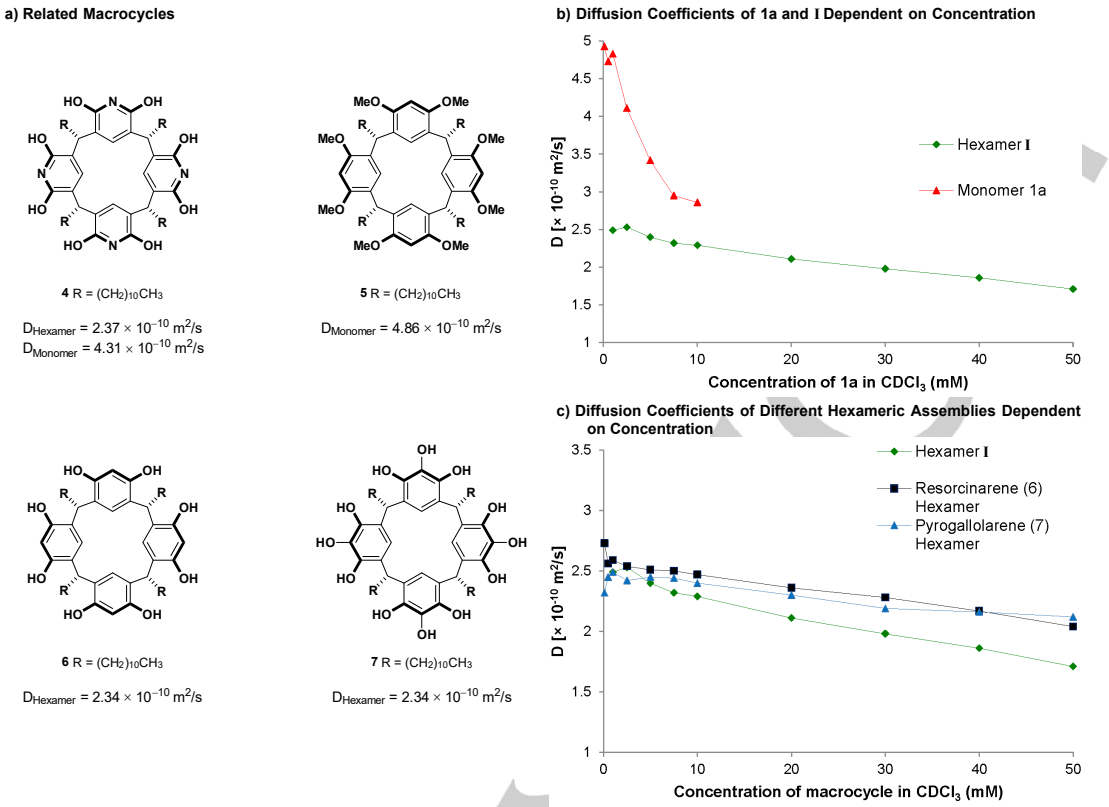

Figure 5. a) Related macrocycles: pyridinearene **4**, octamethylated resorcinarene derivative **5**, resorcinarene **6** and pyrogallarene **7** and their respective diffusion coefficients in $CDCl_3$. b) Concentration dependence of the diffusion coefficients of the monomeric species **1a** and the hexameric species **I** (1 mM – 50 mM in $CDCl_3$). c) Comparison of the diffusion coefficients of the related hexameric assemblies based on macrocycles **1a**, **6** and **7** at different concentrations(1 mM – 50 mM in $CDCl_3$).

EXSY-spectra of a 5.0 mM sample of **1a** in $CDCl_3$, corresponding to a monomer:hexamer ratio of 29:71, were obtained using different mixing times.[21] The results revealed an exchange barrier of 16 – 17 kcal/mol between the two species.[17b]

Assembly **I** was also studied at different temperatures (20 mM in $CDCl_3$) utilizing variable temperature (VT) NMR spectroscopy. While lowering the temperature to −45 °C resulted in considerable broadening and decreasing quality of the spectra, at higher temperatures (up to 55 °C) coalescence of the peaks associated with monomer **1a** and hexamer **I** was observed. This indicates that the peaks are indeed two different species of the same compound, which are in equilibrium.

The results presented above are in agreement with the hypothesis that in chlorinated solvents a dynamic, concentration dependent self-assembly process between monomer and hexamer is observed (Figure 4a). The self-assembly of **I** exhibits a critical aggregation concentration of about 3 mM in $CDCl_3$ (Figure 4c). Once this concentration is reached hexamer **I** is formed in a cooperative fashion while other multimeric species remain undetectable at least by NMR spectroscopy. Based on this conclusion the association constant K_a between monomer **1a** and hexamer **I** can be formulated as:

$$K_a = \frac{[\text{Hexamer}]}{[\text{Monomer}]^6}$$

and was found to be 6.12 ± 1.35 × 10^{13} mol^{-5}•L^5 in $CDCl_3$.

Finally, assembly **I** was investigated concerning its host–guest chemistry. Supramolecular structures have been used in the past to selectively bind fullerenes for separation purposes and to modulate the electronic properties of fullerenes.[2c, 22] To our delight the spherical C_{60}- and C_{70}-fullernes proved to be suitable guest molecules for cage **I** (Table 1, Entry 1 and 2) most likely due to favorable dispersive interactions and potentially π–π-interactions with the cage walls. The encapsulation of C_{60} within the cavity of cage **I** was indicated by a downfield shift of the C_{60}-carbon signal in the ^{13}C-NMR spectra in $CDCl_3$. Due to the low solubility of C_{60} in $CDCl_3$ or potentially as a result of fast guest exchange on the time scale of ^{13}C-NMR we were unable to observe a second signal corresponding to nonencapsulated C_{60}, even in the presence of excess guest. Using C_{70} in toluene-d_8 in the presence of **I** similar results were obtained. The low solubility and the absence of slow exchange prevented the determination of binding constants by ^{13}C-NMR. Due to the low concentrations required for UV/Vis-spectroscopy that prevent the self-assembly of **I**, this technique was also not applicable. To still gain some insight into the encapsulation process by NMR spectroscopy, the soluble ethyl and *tert*-butyl malonyl derivatives of C_{60} and C_{70} were synthesized. The encapsulation of these derivatives was indicated by the appearance of a second set of upfield shifted signals (slow exchange) in the ^{1}H-NMR in presence of **I**. Since only one set of well-defined guest signals was observed, a 1:1 binding mode was assumed. Additional evidence for encapsulation was provided by DOSY-NMR experiments showing similar diffusion coefficients for host **I** and the encapsulated guest molecules (see SI). Association constants were accordingly

determined from the integrals of free and encapsulated guest. The binding constants were found to range from 750 to 2220 M^{-1} (Entry 3 – 6) with C_{60}-derivatives binding slightly stronger than the corresponding C_{70}-derivatives. Contrastingly, in presence of the hexameric resorcinarene and pyrogallolarene capsules no indication for the encapsulation of C_{60}((CH(CO_2Et)$_2$) was observed. These results are interpreted as additional evidence for the formation of a large, discrete cage **I**, which is able to accommodate large, spherical molecules.

Table 1. Encapsulation of guest molecules within assembly **I**.

Entry	Guest[a]	K_a [M^{-1}]
1	C_{60}	n. d.[b]
2	C_{70}	n. d.[b]
3	C_{60}(CH(CO_2Et))	2220[c]
4	C_{60}(CH(CO_2*t*Bu))	790[c]
5	C_{70}(CH(CO_2Et))	910[c]
6	C_{70}(CH(CO_2*t*Bu))	750[c]

[a] **1a**:guest ratio = 6:1 or 12:1, **1a** 20 mM in $CDCl_3$, 16h @ 50 °C;
[b] n. d. = not determined due to low solubility;
[c] determined by ^{1}H-NMR integration.

Although the results of the DOSY-NMR measurements and the binding motif observed in the solid state (Figure 2b) indicate the formation of the larger cage-like structure **I**, we decided also to investigate the energy differences between the two possible hexameric assemblies **I** and **II** with computational methods. According to our gas-phase calculations, the cage structure **I** is lower in energy by 4.5 – 17.2 kcal/mol than the alternative closed-shell structure **II**, depending on the DFT method and the basis set used (Table S8). Also in chloroform, an energy preference for structure **I** in the range of 1.8 – 14.0 kcal/mol was observed (Table S9). This energetic difference may be a result of stronger interunit hydrogen bonds formed in the cage structure **I**. Both the cage **I** and closed-shell structure **II** have 24 interunit hydrogen bonds, but these are shorter in the former by 0.04 − 0.05 Å, depending on the DFT method used (Table S10). These results are fully in line with the experimental findings of this study.

Conclusion

In summary, we have presented the rational design and synthesis of a new supramolecular assembly based on hydrogen bonding. Cage **I** spontaneously self-assembles in chloroform and other chlorinated solvents based on intermolecular amide–amide hydrogen bonding as evidenced by detailed NMR studies and indicated by solid state structures. With an internal cavity volume of approximately 2800 Å^3 cage **I** represents, to the best of our knowledge, the largest capsule/cage structure to date solely based on hydrogen bonding. Comparative DFT studies revealed a significant energy difference between two possible hexameric structures clearly favoring the self-assembly of **I**. The investigation of the properties of assembly **I** in apolar solvents revealed a strong concentration dependence of the self-assembly process and an affinity for fullerenes, which are encapsulated with moderate binding constants. Remarkably, cage **I** is held together by only 24 intermolecular hydrogen bonds all based on simple amide−amide dimerization, while most other assemblies of this class feature a much more complex hydrogen bond network. Furthermore, it features large openings commonly associated with covalently linked cages but unusual for hydrogen-bonded assemblies. We believe that porous structures such as the one presented could potentially be advantageous as they offer an additional handle for further modifications and/or alternative binding sites to obtain heteroassemblies. In general, the simplification of the binding pattern achieved here is expected to aid rational development of future systems and we are confident that the results presented here will help to design new, more sophisticated assemblies in order to overcome the current limitations concerning size and encapsulation of large molecules within hydrogen bonded structures.

Acknowledgements

This work was supported by funding from the European Research Council Horizon 2020 Programme (ERC Starting Grant 714620 – TERPENECAT) and the Swiss National Science Foundation as part of the NCCR Molecular Systems Engineering. We thank PD Dr. Daniel Häussinger and Fabian Bissegger for assistance with the DOSY-NMR and VT-NMR measurements as well as Dr. Michael Pfeffer for HR-MS analysis. L. C. thanks JSPS and the Alexander von Humboldt Foundation for a postdoctoral fellowship. This work was also supported by a grant from the Israeli Science Foundation (Grant 1683/18) (DTM)

Keywords: Supramolecular Chemistry • Self-assembly • Host-Guest Complex

References

[1] For reviews see: a) L. Avram, Y. Cohen, J. Rebek, Jr., *Chem. Commun.* **2011**, *47*, 5368-5375; b) D. Ajami, J. Rebek, Jr., *Acc. Chem. Res.* **2013**, *46*, 990-999; c) L. Adriaenssens, P. Ballester, *Chem Soc Rev* **2013**, *42*, 3261-3277; d) L. J. Liu, J. Rebek, in *Hydrogen Bonded Supramolecular Structures* (Eds.: Z.-T. Li, L.-Z. Wu), Springer Berlin Heidelberg, Berlin, Heidelberg, **2015**, pp. 227-248.

[2] For recent examples see: a) D. Rackauskaite, K. E. Bergquist, Q. Shi, A. Sundin, E. Butkus, K. Warnmark, E. Orentas, *J. Am. Chem. Soc.* **2015**, *137*, 10536-10546; b) D. Beaudoin, F. Rominger, M. Mastalerz, *Angew. Chem. Int. Ed.* **2016**, *55*, 15599-15603; c) G. Markiewicz, A. Jenczak, M. Kolodziejski, J. J. Holstein, J. K. M. Sanders, A. R. Stefankiewicz, *Nat. Commun.* **2017**, *8*, 15109; d) A. Kiesila, N. K. Beyeh, J. O. Moilanen, R. Puttreddy, S. Gotz, K. Rissanen, P. Barran, A. Lutzen, E. Kalenius, *Org. Biomol. Chem.* **2019**, *17*, 6980-6984; e) K. Eichstaedt, K. Szpotkowski, M. Grajda, M. Gilski, S. Wosicki, M. Jaskolski, A. Szumna, *Chem. Eur. J.* **2019**, *25*, 3091-3097; f) H. Jedrzejewska, A. Szumna, *Chem. Sci.* **2019**, *10*, 4412-4421; g) Y. S. Park, Y. Kim, K. Paek, *Org. Lett.* **2019**, *21*, 8300-8303.

[3] a) N. K. Beyeh, F. Pan, K. Rissanen, *Angew. Chem. Int. Ed.* **2015**, *54*, 7303-7307; b) O. Dumele, N. Trapp, F. Diederich, *Angew. Chem. Int. Ed.* **2015**, *54*, 12339-12344; c) L. Turunen, U. Warzok, R. Puttreddy, N. K. Beyeh, C. A. Schalley, K. Rissanen, *Angew. Chem. Int. Ed.* **2016**, *55*, 14033-14036; d) O. Dumele, B. Schreib, U. Warzok, N. Trapp, C. A. Schalley, F. Diederich, *Angew. Chem. Int. Ed.* **2017**, *56*, 1152-1157; e) L. Turunen, A. Peuronen, S. Forsblom, E. Kalenius, M. Lahtinen, K. Rissanen, *Chem. Eur. J.* **2017**, *23*, 11714-11718.

[4] a) C. L. Gibb, B. C. Gibb, *J. Am. Chem. Soc.* **2004**, *126*, 11408-11409; b) A. Suzuki, K. Kondo, M. Akita, M. Yoshizawa, *Angew. Chem. Int. Ed.* **2013**, *52*, 8120-8123; c) J. H. Jordan, B. C. Gibb, *Chem Soc Rev* **2015**, *44*, 547-585; d) A. Suzuki, M. Akita, M. Yoshizawa, *Chem. Commun.* **2016**, *52*, 10024-10027.

[5] a) G. Zhang, M. Mastalerz, *Chem Soc Rev* **2014**, *43*, 1934-1947; b) M. Mastalerz, *Acc. Chem. Res.* **2018**, *51*, 2411-2422; c) M. A. Little, A. I. Cooper, *Adv. Funct. Mater.* **2020**, 1909842; d) T. Hasell, A. I. Cooper, *Nat. Rev. Mater.* **2016**, *1*, 16053.

[6] a) M. J. Wiester, P. A. Ulmann, C. A. Mirkin, *Angew. Chem. Int. Ed.* **2011**, *50*, 114-137; b) T. R. Cook, Y. R. Zheng, P. J. Stang, *Chem. Rev.* **2013**, *113*, 734-777; c) S. H. Leenders, R. Gramage-Doria, B. de Bruin, J. N. Reek, *Chem Soc Rev* **2015**, *44*, 433-448; d) D. Zhang, T. K. Ronson, J. R. Nitschke, *Acc. Chem. Res.* **2018**, *51*, 2423-2436; e) C. M. Hong, R. G. Bergman, K. N. Raymond, F. D. Toste, *Acc. Chem. Res.* **2018**, *51*, 2447-2455; f) M. Yoshizawa, L. Catti, *Acc. Chem. Res.* **2019**, *52*, 2392-2404.

[7] a) D. Fujita, Y. Ueda, S. Sato, H. Yokoyama, N. Mizuno, T. Kumasaka, M. Fujita, *Chem* **2016**, *1*, 91-101; b) D. Fujita, Y. Ueda, S. Sato, N. Mizuno, T. Kumasaka, M. Fujita, *Nature* **2016**, *540*, 563-566.

[8] a) K. Muller-Dethlefs, P. Hobza, *Chem. Rev.* **2000**, *100*, 143-168; b) P. A. Wood, F. H. Allen, E. Pidcock, *CrystEngComm* **2009**, *11*, 1563-1571.

[9] C. Gaeta, C. Talotta, M. De Rosa, P. La Manna, A. Soriente, P. Neri, *Chem. Eur. J.* **2019**, *25*, 4899-4913.

[10] L. R. MacGillivray, J. L. Atwood, *Nature* **1997**, *389*, 469-472.

[11] T. Gerkensmeier, W. Iwanek, C. Agena, R. Frohlich, S. Kotila, C. Nather, J. Mattay, *Eur. J. Org. Chem.* **1999**, *1999*, 2257-2262.

[12] a) X. Liu, Y. Liu, G. Li, R. Warmuth, *Angew. Chem. Int. Ed.* **2006**, *45*, 901-904; b) X. Liu, R. Warmuth, *J. Am. Chem. Soc.* **2006**, *128*, 14120-14127; c) J. Sun, R. Warmuth, *Chem. Commun.* **2011**, *47*, 9351-9353.

[13] K. Kobayashi, M. Yamanaka, *Chem Soc Rev* **2015**, *44*, 449-466.

[14] M. Wierzbicki, A. A. Glowacka, M. P. Szymanski, A. Szumna, *Chem. Commun.* **2017**, *53*, 5200-5203.

[15] C. Schäfer, J. Mattay, *Photochem. Photobiol. Sci.* **2004**, *3*, 331-333.

[16] R. Taylor, O. Kennard, W. Versichel, *Acta. Crystallogr. B* **1984**, *40*, 280-288.

[17] a) H. C. Chen, S. H. Chen, *J. Phys. Chem.* **1984**, *88*, 5118-5121; b) A. Macchioni, G. Ciancaleoni, C. Zuccaccia, D. Zuccaccia, *Chem Soc Rev* **2008**, *37*, 479-489.

[18] a) L. Avram, Y. Cohen, *Org. Lett.* **2002**, *4*, 4365-4368; b) L. Avram, Y. Cohen, *Org. Lett.* **2003**, *5*, 3329-3332; c) T. Evan-Salem, Y. Cohen, *Chem. Eur. J.* **2007**, *13*, 7659-7663.

[19] M. H. Abraham, R. J. Abraham, W. E. Acree, Jr., A. E. Aliev, A. J. Leo, W. L. Whaley, *J. Org. Chem.* **2014**, *79*, 11075-11083.

[20] a) J. R. Neale, N. B. Richter, K. E. Merten, K. G. Taylor, S. Singh, L. C. Waite, N. K. Emery, N. B. Smith, J. Cai, W. M. Pierce, Jr., *Bioorg. Med. Chem. Lett.* **2009**, *19*, 680-683; b) D. Joarder, S. Gayen, R. Sarkar, R. Bhattacharya, S. Roy, D. K. Maiti, *J. Org. Chem.* **2019**, *84*, 8468-8480.

[21] S. Y. Chang, H. Y. Jang, K. S. Jeong, *Chem. Eur. J.* **2003**, *9*, 1535-1541.

[22] a) S. J. Park, O. H. Kwon, K. S. Lee, K. Yamaguchi, D. J. Jang, J. I. Hong, *Chem. Eur. J.* **2008**, *14*, 5353-5359; b) N. Kishi, M. Akita, M. Kamiya, S. Hayashi, H. F. Hsu, M. Yoshizawa, *J. Am. Chem. Soc.* **2013**, *135*, 12976-12979; c) J. Camacho Gonzalez, S. Mondal, F. Ocayo, R. Guajardo‐Maturana, A. Muñoz‐Castro, *Int. J. Quantum Chem.* **2019**, *120*, e26080; d) X. Chang, S. Lin, G. Wang, C. Shang, Z. Wang, K. Liu, Y. Fang, P. J. Stang, *J. Am. Chem. Soc.* **2020**.

Entry for the Table of Contents

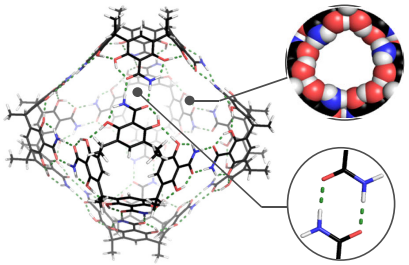

- Large Cage Structure (V ≈ 2800 Å^3)
- Concentration-dependent Self-assembly *via* Dimerization of Amides

A large, hexameric cage based on amide dimerization self-assembles from a designed macrocyclic building block in apolar solvents. The unusually large structure (V ~ 2800 Å^3) features openings commonly associated with covalently linked cages and forms host–guest complexes with fullerenes (C_{60} and C_{70}). The formation of the hexameric structure was found to be strongly concentration dependent.

Institute and/or researcher Twitter usernames: @TiefenbacherLab